JJMIE

Volume 8 Number 5, October 2014
ISSN 1995-6665
Pages 265 - 274

Jordan Journal of Mechanical and Industrial Engineering

The Effects of Content and Surface Modification of Filler on the Mechanical Properties of Selective Laser Sintered Polyamide12 Composites

Alkhair A. Mousa *

Technology Collage of Engineering, Department of Mechanical Engineering, Houn-Libya

Received 3 Sep 2014 *Accepted 25 Oct 2014*

Abstract

In selective laser sintering, the mechanical properties of the sintered part are largely influenced by many factors such as powder material, processing parameters, fabrication position and orientation. The present paper investigates the influence of content and surface modification of glass beads on the mechanical properties. The aim is particularly to better understand the effect of coupling agents on the mechanical properties of laser sintered parts. The specific material of interest is Polyamide 12 filled with two types of A-glass beads. The production of test specimens is carried out on a DTM Sinterstation 2000 Machine. Quasi-static mechanical tests are used to examine the mechanical properties of selective laser sintered specimens. The results show that adding glass beads (coated/ un-coated) to Polyamide 12 improves the tensile strength and elastic modulus but reduces the impact strength and ductility of the sintered parts.

Keywords: *: Selective Laser Sintering, Polyamide 12, Coupling Agents, Glass Beads*.

1. Introduction

Although the use of fillers in plastics industry has been known for several decades, there is still an enormous interest in all the fields of the development of composite materials with enhanced properties. Mineral fillers are added to the polymers in commercial production primarily for reasons related to cost reduction and properties improvement. Improving the existing materials and developing new materials for use in Selective Laser Sintering (SLS) are continually being pursued in the industrial and academic domains [1].

The use of polymeric materials in the SLS process offers some advantages over metallic and ceramic materials, which are related to the low processing temperature, melting flow control and high corrosion resistance. However, the variety of commercial polymeric materials available for SLS process is restricted, and this reduces the options available during material selection for manufacturing particular parts. The use of available non-commercially polymers and mixtures of polymers can increase the range of properties of SLS parts [2].

Thermoplastics, such as polycarbonate and polyamide, have been developed as SLS materials for different applications. However, these materials cannot completely meet the needs of different functional end use parts. In recent years, the modification and improvement of physical properties of pure polyamide by adding inorganic fillers (such as clays, talc, silica, glass bead, wollastonite and kaolin, etc.) have received close attention.

Glass beads-filled polyamide composites have become attractive due to their low cost and widespread applications in automobile, aerospace and electrical industries. The modification of the surface of glass beads is essential to improving surface wetting and adhesion between the filler and matrix. This may be improved by chemically incorporating specific interaction sites onto the glass beads surface or coating it with reactive surfactants or coupling agents [3].

In this study, glass beads (GB), by weight ratios wt%, were added to Polyamide12 (PA 12, PA2200). The influence of the addition of glass beads on the mechanical properties of the specimens produced under predetermined processing parameters was examined.

2. Previous work on the relationship between part properties, fillers and process parameters in SLS

Numerous attempts have been made to study the effect of powder material and process parameters on mechanical properties of SLS parts. The influence of fabrication parameters on the properties of SLS parts has been investigated by Gibson and Shi [4] who showed that the mechanical properties vary when different powders are used if similar process parameters are selected. They

* Corresponding author. e-mail: alkhair_brno@yahoo.com.

concluded that, besides powder material properties, fabrication parameters, orientation and building position also influence the mechanical properties. Wong *et al.* [5] studied the SLS of blended powder from PA12 and organically modified rectorite (OREC). Compared with pure PA12, the results of this investigation showed that the laser power needed for sintering greatly decreased and the mechanical properties of the sintered samples considerably improved with the addition of OREC (0-5 wt%). Experimental investigations into the production of particulate silicon carbide (SiC) polyamide matrix composites using the selective laser sintering process have been conducted by Gill *et al.* [6]. Their investigation revealed that the optimum energy density for producing samples of maximum strength was independent of the initial powder blend composition. For SLS applications, Mozzoli *et al.* [7] developed and characterized a new aluminium-filled polyamide powder from a rheological perspective. They reported that the new material allowed SLS manufacturing of models with considerably high dimensional accuracy, strength and resistance to mechanical stresses. A study of mechanical anisotropy due to build orientation and the end-of-vector effects in the laser sintering process was presented by Ajoku *et al.* [8]. The results of the tests showed that the build orientation of the samples had an effect on the mechanical properties obtained. They concluded that the orientation of a part in the laser sintering machine is the primary variable which affects its mechanical properties and the end-of-vector effect is a secondary factor, which is more prominent in parts with small x dimensions. A paper investigating the mechanical properties of parts produced via SLS has been published by Caulfield *et al.* [9]. They investigated the influence of several process parameters on the physical and mechanical properties of polyamide 12 parts. They generally showed that the mechanical properties of parts are highly dependent on process parameters and part orientations. Experimental investigations have been made by Jain *et al.* [10] to understand the effect of the delay time on part strength in selective laser sintering. They successfully developed an algorithm and implemented it to predict part orientation for the improved part strength by considering delay time. They concluded that comparatively higher strength can be achieved by orienting the part so that the maximum area on all layers falls within the optimum delay time range. Another experimental investigation was carried out by Jain *et al.* [11] to study the feasibility of processing blended powder of polyamide (PA) and organically modified nanoclay using SLS process. The authors found that the addition of clay did not improve the mechanical properties of the laser sintered polyamide; rather, it resulted in decreased mechanical properties. Goodridge *et al.* [12] have presented initial research into the reinforcement of laser sintered polyamides with carbon nanofibres (CNF). They investigated the effects of CNF addition on the processing parameters and mechanical properties of laser sintered parts and demonstrated that CNF can increase the strength of a base polyamide 12 laser sintering polymer prepared using a melt-mixing technique. They reached the conclusion that the nanofibres were well-dispersed within the polymer matrix and increased the storage modulus compared to the base material. Improvements to the production of the nanocomposite starting powder were required to use these materials effectively with laser sintering.

However, none of the abovementioned studies considered the mechanical properties of laser sintered PA 12 parts by investigating the relationship between surface pre-treated filler and, in particular, the effect of coupling agents on the mechanical properties of selective laser sintered glass bead-filled polyamide 12 composites. Currently, to the best of our knowledge, no such studies have been conducted on PA 12/GB composites processed using the SLS technique. The present paper is the first attempt to address this issue by experimentally analyzing the influence of coupling agents on the mechanical properties of sintered components in polyamide 12 composites.

3. Coupling Agents

The adhesion between polymeric materials and particulate fillers is usually weak due to the poor compatibility of the polymer with the mineral surface. To improve the compatibility, adhesion promoters are commonly required. The most widely used of these are the silane coupling agents with the general structure (RO)3SiY, where RO is an alkoxy group and Y is an organo-functional group [13], as shown in Figure 1:

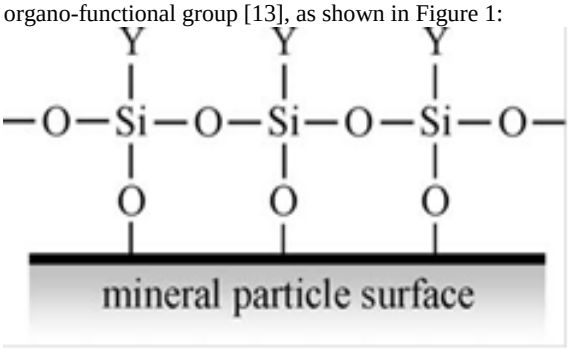

Figure 1. Idealistic view of a silane-treated surface [13]

Silane is a molecule containing a central silicon atom bonded to two types of groups: Alkoxy groups and organo-functional groups. These two types exhibit different reactivity and allow sequential reactions. In the crosslinking process, the first step is generally the grafting of the silane the polymer backbone via condensation of silanols. Silane coupling agent will act in this case as a link between an inorganic substrate and an organic material to bond, or couple, the two dissimilar materials together. Figure 2 shows a simplified picture of the coupling mechanism [14]:

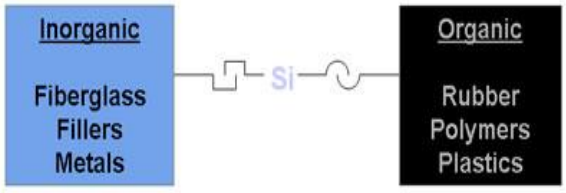

Figure 2. Silane coupling mechanism [14]

The main role of the coupling agents is to promote adhesion which will result in developing the mechanical properties, such as tensile and flexural strength, fracture toughness, tensile modulus, etc. [15].

4. Experimental Procedures

4.1. Materials and Processing

Polyamide 12 powder, used in this study, was a commercial fine polyamide (PA 2200) supplied by EOS GmbH with average grain size of 60 μm. The density, according to DIN EN ISO 60 (2000-01) was 0.435 to 0.445 g.cm^{-3}.

Two A-glass beads (Spheriglass: 3000CP00 no surface modification and 3000CP03 surface modified with a silane coupling agents) with mean diameter of 35 μm were selected as filler, Figure (3). The glass beads, small solid spherical particles with a density of 2.5 g.cm^{-3}, were supplied by Potters Industrial Inc/Omya UK Ltd.

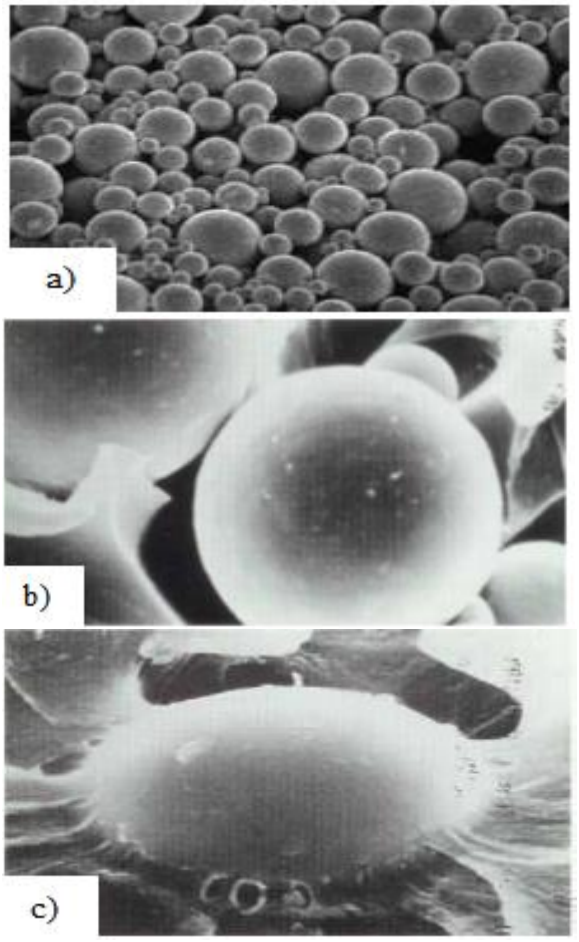

Figure 3. Spheriglass, A Glass: a) Solid Glass Spheres; b) Uncoated; c) with coating [16]

4.2. Specimens Preparation

In specimens preparation process, pure PA12 was compounded with (GB) with 10, 20, 30 and 40wt% ratios, using a rotating drum mixer (type BS125) for 30 min to produce the composites.

Selective laser sintering process was performed, under predetermined processing parameters, using a SLS machine to manufacture the specimens of PA12/GB composites with: fill laser power of 10W; laser beam speed of 914mm/s; scan spacing of 0.15mm; layer thickness of 0.10mm; beam diameter of 0.40mm and powder bed temperature of 176 °C. The energy density, regarded as the relative applied laser energy per unit area, can be calculated as follows [9]:

$$ED = \frac{LP}{BS \; x \; SCSP} \quad (1)$$

Therefore, the corresponding laser energy density is 0.073 J/mm^2. Table 1 summarises the optimum process parameters used in manufacturing of test specimens from the PA12/GB composites.

Table 1. Optimized processing parameters used in manufacturing of test specimens

PA12/GB [wt/wt%]	90/10	80/20	70/30	60/40
Laser power; LP [W]	10			
Energy density; ED [J/mm^2]	0.073			
Beam Speed; BS [mm/s]	914			
Powder bed temperature; T_b [°C]	176			
Scan Spacing; SCSP [mm]	0.15			

4.3. Equipment and Methodology

In the testing step, the tensile, flexural and Izod impact specimens according to BS EN ISO 527, 178 and 180/1A standards were produced using SLS machine. In order to maintain consistency in this study, all specimens were built flat, laid parallel to the direction of the movement of the roller, and at fixed places in the middle of the build area as shown in Figure 4.

The tensile, flexural and fracture toughness tests were carried out using Testometric materials testing machine. The impact test was carried out at room temperature using pendulum impact test machine type W&T AVERY LTD.

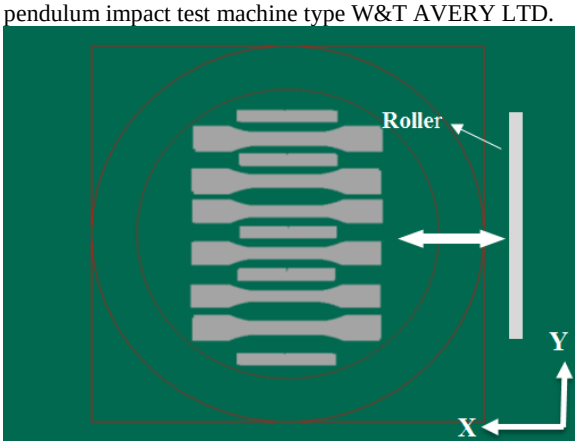

Figure 4. Orientation of the specimens in the build platform (Top view)

The tensile strength, elastic modulus, elongation at break, impact strength, flexural strength and fracture toughness were recorded and obtained. For the morphological observations a Scanning Electron Microscope (SEM) type (ZEISS XB 1540 workstation) was used to observe the morphology of scan surfaces and the fracture cross- section of tensile bars.

5. Results and Discussion

5.1. Density Measurements of Sintered Density Specimens

The density of selective laser sintered components has an important influence on the mechanical properties and a nearly full relative density is one of the most important properties required for functional parts. Therefore, the density prediction of SLS parts provides suitable guidelines in the selection of appropriate process parameters as seen in Figure 5.

The density of the sintered specimens from the PA12/GB composites was predicted by building density specimens. These density specimens were small square prisms with the intended dimensions of 20mm x 20mm x 5mm. Once the density specimens were built, their dimensions were determined manually by measuring with a digital caliper and they were weighed. The average density of the sintered specimens was 0.92 g/cm^3 obtained from six measurements as shown in Table 2.

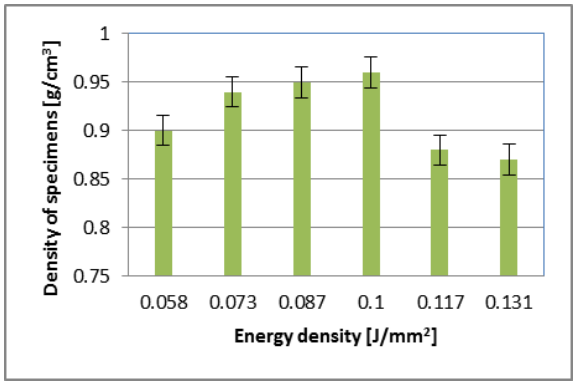

Figure 5. Influence of energy density on the density of sintered density specimens

Table 2. Measured data of the sintered density specimens

Energy density [J/mm^2]	*l* [mm]	*w* [mm]	*h* [mm]	*m* [g]	V [mm^3]	P [g/cm^3]
0.058	20.64	20.64	5.74	2.2	2445.3	0.90
0.073	20.46	20.46	5.56	2.2	2327.5	0.94
0.087	20.24	20.24	5.40	2.1	2212.1	0.95
0.100	20.04	20.04	5.17	2.0	2076.3	0.96
0.117	20.40	20.40	5.48	2.0	2280.5	0.88
0.131	20.43	20.43	5.75	2.1	2400.0	0.87

5.2. Dimensional Measurement of Sintered Test Specimens

The dimensions of the sintered specimens in PA12/GB composites were measured using a digital vernier caliper and listed in Table 3. It is shown that the specimens have a good dimensional accuracy and there were no obvious differences between both systems.

As depicted in Figure 6, the average values were within the intended dimensions. However, it is not difficult to conclude that the dimensional accuracy is material- and machine-dependent; also it is well known that the isotropic behaviour of glass spheres provides uniform shrinkage which is an important factor in the reduction of the dimensional inaccuracy.

Table 3. Measured dimensions of sintered tensile test specimens (PA12/CP03 system)

Energy density [J/mm^2]	0.073				
PA12/CP03 [w%/wt%]	100/0	90/10	80/20	70/30	60/40
Thickness of specimen [mm]	3.990	3.978	3.864	3.934	3.872
Width of specimen [mm]	10.011	10.052	10.352	10.168	10.331
Length of specimen [mm]	150.015	149.754	150.206	150.112	150.177
Average cross-sectional area [mm^2]	39.944	39.987	40.000	40.000	40.002

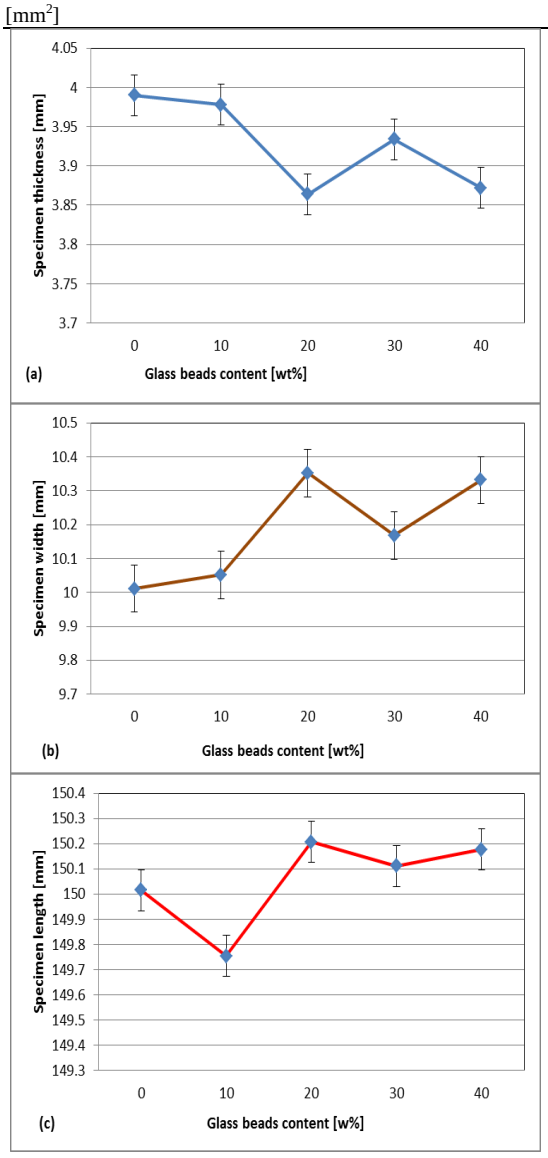

Figure 6. Variation of specimen dimensions with filler ratio: (a) thickness; (b) width; (c) length

5.3. Mechanical Properties

The mechanical properties of the composites (PA12/CP00 and PA12/CP03 systems) were investigated as a function of content and surface modification of glass beads using selective laser sintered test specimens. Optimized process parameters and scale factors for compensation of the shrinkage were applied to all fabricated test specimens.

Tensile Strength

The tensile specimens had a nominal thickness of 4mm, width of 10mm and other dimensions were determined with reference to BS EN ISO 527-2 Type 1A, shown in Figure 7. The as-sintered specimens were tested under ambient conditions and at a crosshead speed of 5 mm/min.

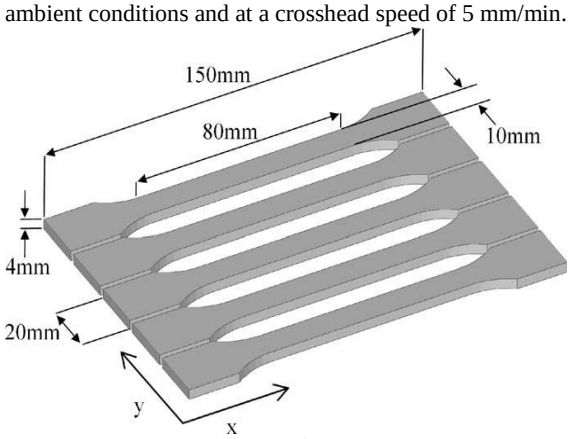

Figure 7. Shape and dimensions of the tensile test specimens

The value of average tensile strength was obtained from six tests. Figure 8 displays the variation of tensile strength of the PA12 composite with glass beads content for both systems.

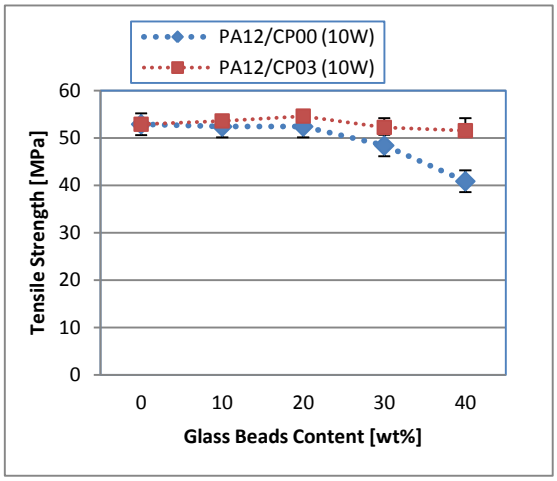

Figure 8. Variation in tensile strength of the composites.

Initially, it is clear that the tensile strength increases with the increase in the glass beads ratio, namely: from 53 MPa at 10 wt% to 55 MPa at 20 wt%. Above 20 wt% the addition of increasing amounts of glass beads led to decrease in the tensile strength. The reduction in the strength may be attributed to the reduction in the adhesion strength between the matrix (PA12) and the aggregate (glass beads) due to less polyamide and increasing structural microporosity. Compared to PA12/CP00 system, the better interfacial adhesion gives higher composite strength in case of surface modified glass beads, PA12/CP03 system.

Elastic Modulus

Modulus of elasticity is the stiffness of material at the elastic stage of tensile test. It markedly improved by adding rigid particles to the polymer matrix since the rigidity of inorganic fillers is generally higher than that of the polymers.

From Figure 9, it can be seen that increasing the ratio of glass beads from 10 to 40 wt% led to a remarkable increase in the elastic modulus from approximately 1974.4 to 3399.6 MPa.

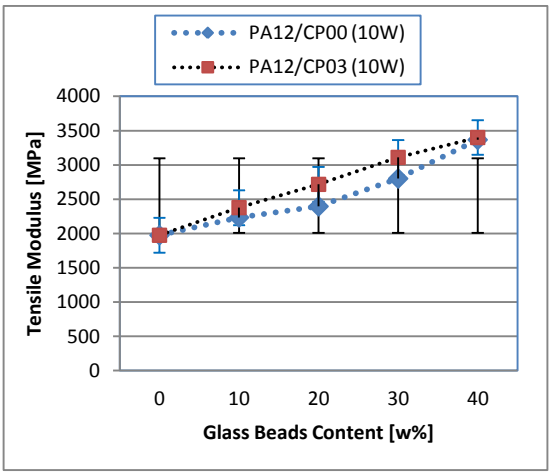

Figure 9. Variation of modulus of elasticity

The changes of the adhesion parameters in the composites as a consequence of the glass beads surface modification are expected to reflect in the changes of the composite mechanical properties. However, there were no obvious differences in the elastic modulus between the PA12/CP00 and PA12/CP03 laser sintered specimens. It is seen that the elastic modulus is independent of the interfacial adhesion between PA12 and GB. However, since elastic modulus is measured at a relatively low deformation, there is insufficient dilation to cause interface separation. Thus, it is easy to understand that the adhesion strength does not noticeably affect the elastic modulus [17].

Elongation at break

As it can be seen from Figure 10 the measured elongation at break with 10 wt% glass beads was 4.18% then decreased to 0.18% at glass beads ratio of 40 wt%. The decrease of elongation at break with the presence of glass beads is generally explained by the immobilisation of the macromolecular chains by the glass beads which increase the brittleness of the PA12 matrix.

In the same way, the lowering of the elongation at break of the composites may be also associated with weak GB/PA12 adhesion. Even though there was a proper interfacial adhesion between GB and PA12, this adhesion appeared unable to withstand the deformations and elongations at rupture of glass beads filled composites failing it catastrophically. Additionally, from the trend in variation in the elongation at break of the PA12/GB composites, it is clear that, as the content of GB increases, the elongation at break decreases considerably.

  - Volume 8, Number 5 (ISSN 1995-6665)

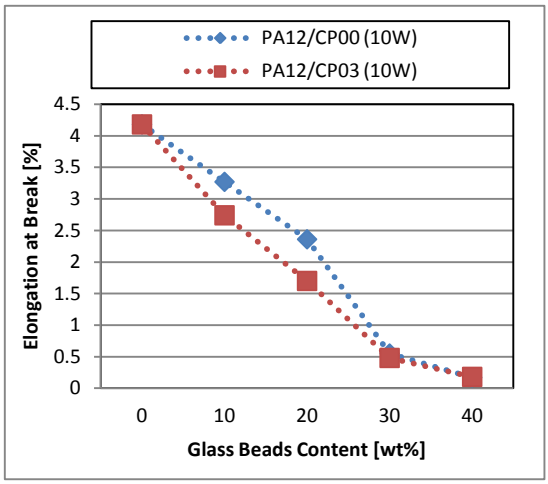

Figure 10. Variation of elongation at break

Flexural Strength and Modulus

Figure 11 shows the variation of the flexural strength and modulus with glass beads content. Flexural strength and modulus were obtained through a three-point bending test. The results from the experiments show that flexural strength increased gradually, whilst the flexural modulus values increased steadily as the glass beads loading increased from 10 to 40 wt%.

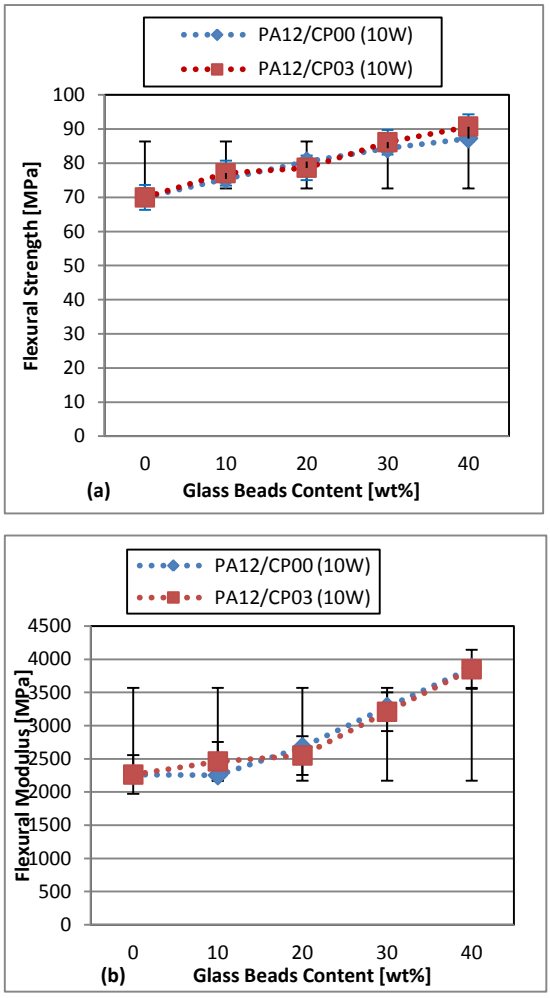

Figure 11. Variation of flexural strength (a) and flexural modulus (b)

However, the flexural strength and flexural modulus values of the PA12/CP03 system were slightly higher than those of the PA12/CP00 system, where, as generally believed, the coupling agent would soften the PA12 matrix around the glass beads which have a smooth spherical surface and should not initiate fine cracks in the matrix around them.

Impact Strength

The impact strength of notched specimens was measured at ambient temperature by the notched Izod test. Izod impact tests were carried out on 80mm x 10mm x 4mm rectangular bars with a single-edge of 45° V-shaped notch (tip radius 0.25 mm, depth 1.5 mm).

The impact strength of different PA12/GB composites with different filler content is shown in Figure 12. It becomes apparent that the impact strength increased to some extent with increased glass beads ratio, particularly at 10 wt%. With loading up to 20 %wt, the significant drop in impact strength was readily apparent. The explanation of this observation is that: for lower contents, glass beads are well- dispersed in the PA12 matrix, the impact energy is more uniformly distributed and the effect is higher impact strength. For higher contents, the decrease in impact strength may be related to the tendency to form glass bead agglomerates, resulting in a poor dispersion of the fillers on the PA12 matrix. Furthermore, the degradation in impact properties can be attributed to the immobilisation of the macromolecular chains by the glass beads which limits their ability to deform freely and reduces the ductility of the composites [18].

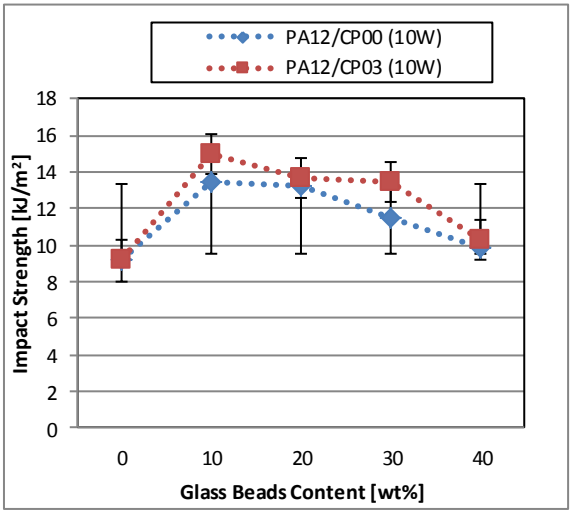

Figure 12. Variation of impact strength

From the impact experiment, it was found that the strengths of both composites decreased monotonically from 14.40 to 9.84 kJm^{-2} with increasing GB weight ratio regardless to surface modification. Table 4 represents the experimental results of mechanical properties of sintered PA12/GB composites.

Table 4. Experimentally obtained mechanical properties of SLS specimens

PA12/ CP00 ratios [wt%]	100/0	90/10	80/20	70/30	60/40
Laser power [W]	10				
Properties; Composite Material: PA12/CP00					
Tensile strength [MPa]	52.89	52.39	52.40	48.40	40.85
Tensile modulus [MPa]	1974.4	2233.8	2395.7	2800.9	3366.5
Ultimate elongation [%]	4.18	3.27	2.36	0.55	0.17
Flexural strength [MPa]	69.97	75.43	80.41	84.38	87.20
Flexural modulus [MPa]	2262.91	2252.98	2675.18	3280.86	3870.03
Impact strength [kJ/m^2]	9.14	13.97	13.18	11.46	9.84
Properties; Composite Material: PA12/CP03					
Tensile strength [MPa]	52.89	53.59	54.61	52.23	51.54
Tensile modulus [MPa]	1974.4	2377.2	2716.5	3110.0	3399.6
Ultimate elongation [%]	4.18	2.74	1.70	0.48	0.18
Flexural strength [MPa]	69.97	77.07	78.61	86.14	90.70
Flexural modulus [MPa]	2262.91	2460.51	2549.98	3208.68	3849.12
Impact strength [kJ/m^2]	9.14	14.40	13.65	13.41	10.29

6. Fracture Toughness

To determine the fracture toughness of the glass beads-filled polyamide12 composites under quasi-static load there are two approaches: the stress intensity approach and the energy approach. The first approach yields fracture toughness (K_c); the second provides a critical energy release rate (G_c). The fracture toughness specimens were produced using a DTM Sinterstation 2000 machine under the same conditions applied to other test specimens. The length (L), thickness (B) and width (*W*) of the specimens were 80mm, 10mm and 4mm, respectively (BS ISO 17281), shown in Figure 13. The single edge V- shaped notches of 45°, with a tip radius of 0.25mm and different depths were introduced using the SLS machine.

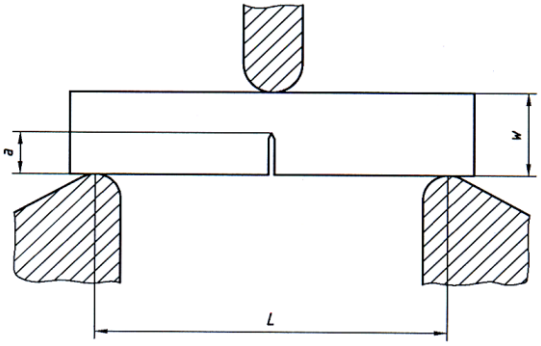

Figure 13. Specimen configuration and dimensions for fracture toughness measurements [19]

Single- Edge- Notched Three- Point Bending Fracture Toughness Tests

It is well known that the toughness tests could also be performed on the composites at slower rate than impact conditions by drawing out the notched rectangular bar specimens. For this purpose, five sets from which five replicate specimens of each were produced and tested at room temperature on a Testometric materials testing machine AX at a cross-head speed of 1 mm/min using a span of 64 mm.

Single-edge-notched (SEN) type specimens were prepared for the determination of the critical stress intensity factor (K_{IC}) in the three-point bending (3PB) test. The obtained load-displacement curves allowed for making statements about the behavior of the composites. An example for the resulting load-displacement curves of the glass beads-filled polyamide composites is given in Figure 14. Looking at the effect of the notch depth on the stress-strain curves of the specimen, it is clear that as the depth increased, the stress and the strain decreased.

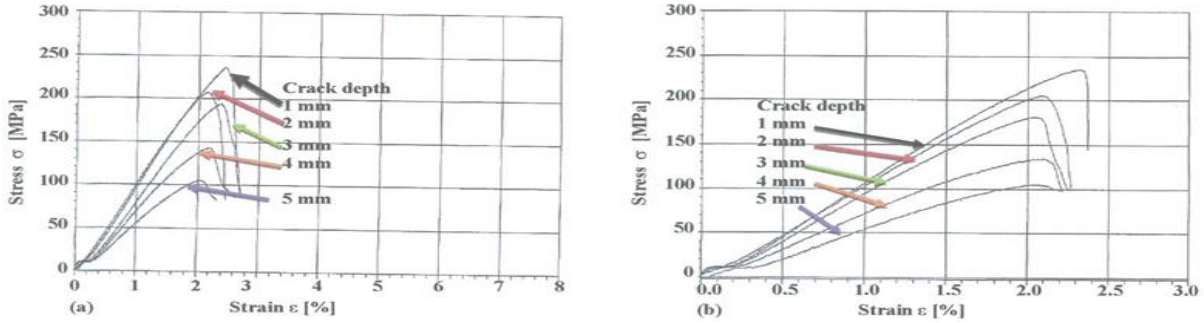

Figure 14: Stress-strain curves for composites containing 20 wt% of glass beads (a) CP00/PA12; (b) CP03/PA12

Correlation between Fracture Toughness and Glass Beads Content

The fracture toughness was studied as a function of glass beads loading. It was found that the toughness reached a maximum at 10 wt% of glass beads and then decreased with more glass beads added.

The dependency of plain strain fracture toughness, i.e., the critical stress intensity factor (K_{IC}) of glass bead-filled polyamide 12 is given in Figure 15. The most distinctive feature in this figure is that the fracture toughness of the both composite systems did not show any significant increase with increasing glass beads content. In fact, it decreased with the increase in glass beads content. In other words, the addition of glass beads led to composites with brittle behavior.

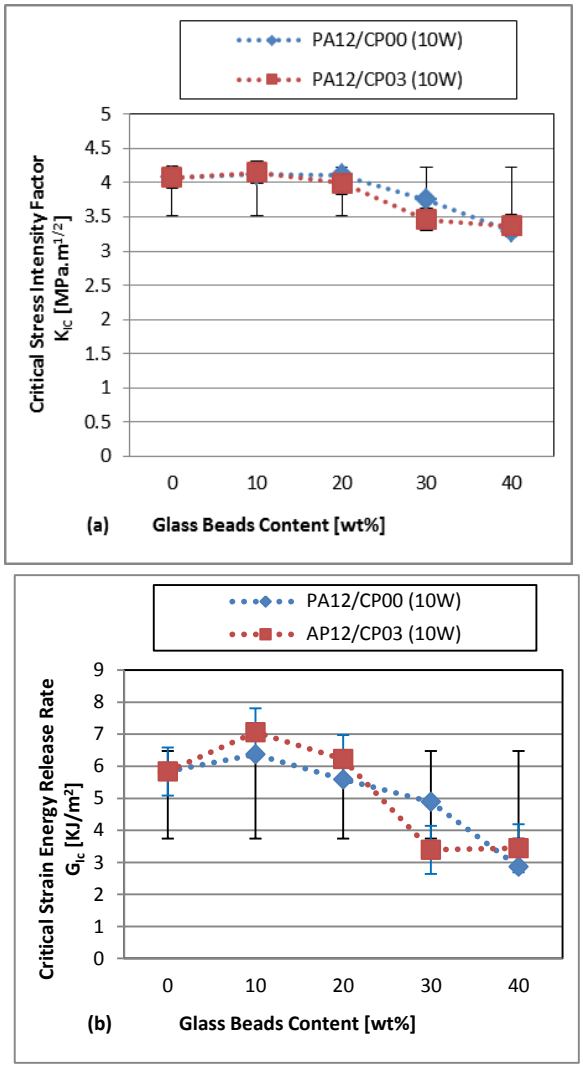

Figure 15. Dependency of fracture toughness of polyamide 12 composites on glass beads content (a) K_{IC}; (b) G_{IC}

From the abovementioned figure, it can be observed that the influence of the surface treatment on fracture toughness is insignificant; therefore, a small amount of energy can be damped via de-bonding. Besides, a crack can propagate through an interface easily because of a weak interface adhesion.

7. Morphological Observations

The effect of the coupling agent on the interfacial adhesion is often evaluated from the micrographs of fractured surfaces. The morphological study included the intrinsic microstructures of the blends of the fractured surfaces after tensile tests. The SEM micrographs of the PA12/ GB composites processed using the optimal parameter sets are shown in Figures 16; 17 and 18.

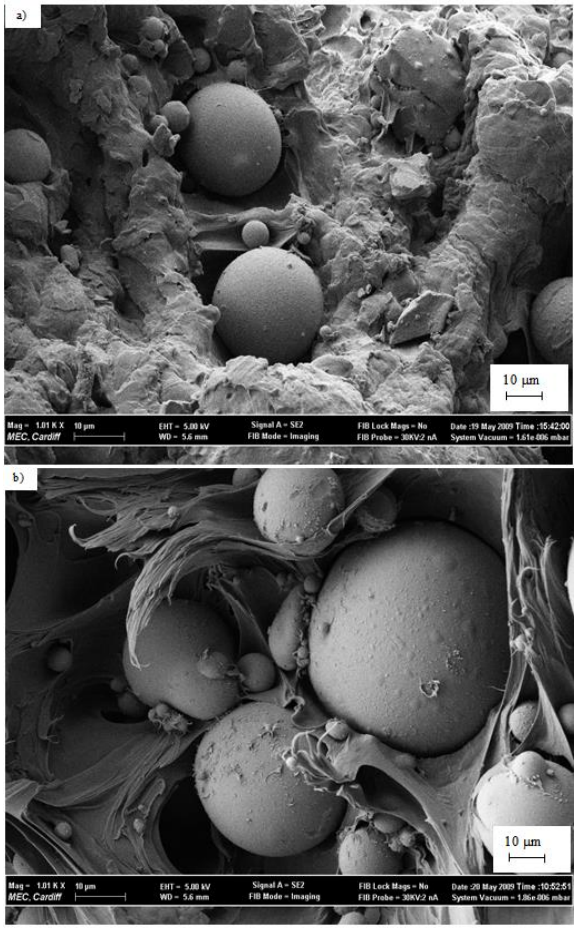

Figure 16. SEM micrographs of tensile fracture surfaces: PA12/CP00 composite containing 20 wt% of glass beads; ED= 0.073 J/mm^2

For PA12/CP00 system (20 wt% at ED= 0.073 J/cm^2), it can be seen from Figure 16(a) and (b) that the connection between the GB and PA12 was not perfect; many glass beads have been pulled out and that PA12 was stretched during breakage, resulting in a rough spongy surface.

The de-bonded glass particles surrounded by the void created due to deformation of the PA12/GB composite. However, the tensile fracture cross-section of the un-treated GB in the composite after de-bonding was relatively smooth and this specifies that the interfacial adhesion was poor between PA12 and GB.

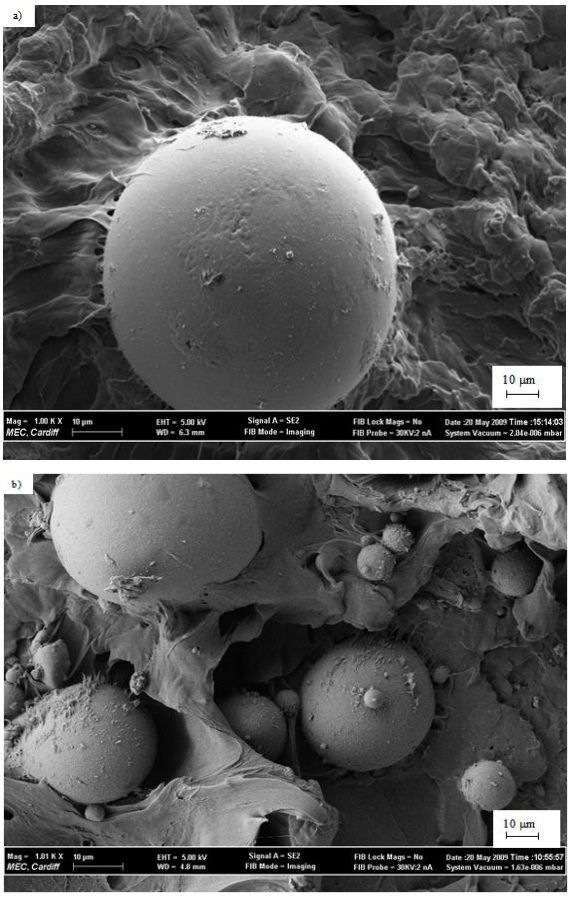

Figure 17. SEM micrographs of tensile fracture surfaces: PA12/CP03 composites containing 20 wt% of glass beads; ED= 0.073 J/mm^2

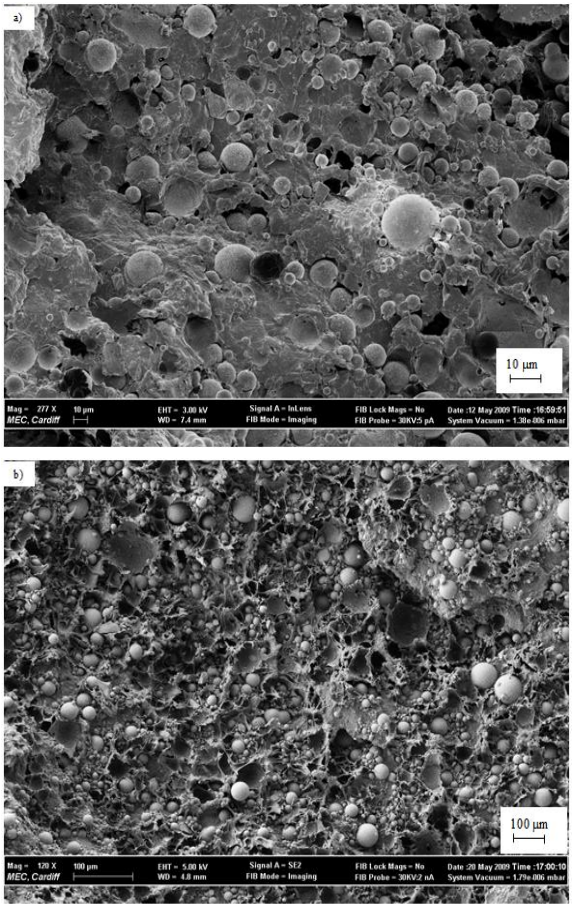

Figure 18. SEM micrographs of tensile fracture surfaces: a) PA12/CP00 and b) PA12/CP03 composites containing 40 wt% of glass beads each; ED= 0.073 J/mm^2

Figure 17 depicts SEM micrographs taken of the tensile fracture cross-sections of the PA12/CP03 system (20 wt% at ED= 0.073 J/cm^2). In this case, the treated beads appear to remain solidly anchored and strongly adhered to the matrix and their surface become relatively rough. Hence, the bonding between the glass beads and the matrix was strengthened. These results indicate that the silane agent coated on the surface of glass beads enhanced the interaction between the PA12 and GB, and improved the adhesion, Figure 17(a) and (b).

The fractured surfaces of Figure 18(a) and (b) represent a kind of median situation for each type of glass bead; they do not provide a completely accurate description of the composite. In fact, it is possible to find in untreated glass beads-polyamide 12 composites a significant proportion of glass bead particles that have not separated from the matrix, see Figure 18(a). Conversely, in surface treated glass bead composites, a significant number of de-bonded particles have been observed, see Figure 18(b).

8. Conclusions

In the present work, an attempt has been made to study the effects of content and surface modification of glass beads on the mechanical properties of SLS parts fabricated from polyamide 12 composites. Under predetermined processing parameters, several mechanical properties, such as tensile strength, elasticity modulus, elongation at break, flexural strength and modulus, impact strength, fracture toughness and microstructural properties of PA12/GB composites, were investigated. The following results can be drawn from the experimental results:

- The strength of PA12/GB composites is generally affected by PA12/GB interface adhesion and glass beads content. Initially, it increased with the increase in the glass beads ratio from 53MPa at 10 wt% to 55 MPa at 20 wt%; then decreased above 20 wt%.
- Regardless of the surface modification, elastic modulus increased considerably from 2000 to 3400 MPa as the glass beads content increased.
- In both systems, the elongation at break decreased steadily as the glass beads content increased, namely from 2.74% at 10 wt% to 0.18% at glass beads ratio of 40 wt%.
- There was a significant increment in the flexural properties with an increase in the beads loading. The flexural strength increased gradually (77 to 91 MPa), whilst the flexural modulus values increased steadily (2500 to 3800 MPa) as the glass beads ratio increased (10 to 40wt%).
- The impact strengths of both composites decreased monotonically (14 to 10 kJm−2) with increasing GB weight ratio regardless of the surface modification. The significant drop in impact strength was readily apparent with loading up to 20 %wt.
- The fracture toughness of PA12/GB composites was observed to peak slightly at low glass beads content and then decreased with more beads added. Regardless of the surface modification, increasing notch depth leads to a decrease in the fracture toughness.
- SEM micrographs of fracture surfaces showed that PA12 was pulled away from uncoated GB as the test specimen was stretched whereas it was strongly adhered to the surface modified GB.

Important Note

This research received no specific grant from any funding agency in the public, commercial, or not-for-profit sectors.

References

[1] I. Švab, V. Musil, M. Leskovac: "The Adhesion Phenomena in Polypropylene/ Wollastonite Composites". Acta Chim. Slov. Vol. 52 (2005) 264–271.

[2] G. V. Salmoria, J. L. Leite, R. A. Paggi, A. Lago, A. T. N. Pires: "Selective laser sintering of PA12/HDPE blends: Effect of components on elastic/plastic behaviour". Polymer Testing, Vol. 27 (2008) No. 6, 654-659.

[3] H. Unal: "Morphology and mechanical properties of composites based on polyamide 6 and mineral additives". Materials and Design, Vol. 25 (2004) 483 – 487.

[4] I. Gibson, D. Shi: "Material properties and fabrication parameters in selective laser sintering process". Rapid Prototyping Journal, Vol. 3 (1997) No. 4, 129 – 136.

[5] Y. Wang, Y. Shi, S. Huang: "Selective laser sintering of polyamide-rectorite composite". Proceedings of the Institution of Mechanical Engineers, Part L: Journal of Materials Design and Applications January, Vol. 1 (2005) No. 219, 11-15.

[6] T. J. Gill, K. K. B Hon: "Experimental investigation into the selective laser sintering of silicon carbide polyamide composites". Proceedings of the Institution of Mechanical Engineers, Part B: Journal of Engineering Manufacture October 1, (2004) No. 218, 1249-1256

[7] A. Mazzoli, G. Moriconi, M. G. Pauri: "Characterization of an aluminum filled polyamide powder for applications in selective laser sintering". Materials & Design, Vol. 28 (2007) No. 3, 993-1000.

[8] U. Ajoku, N. Saleh, N. Hopkinson, R. Hague, P. Erasenthiran: "Investigating mechanical anisotropy and end-of-vector effect in laser-sintered nylon parts". Proceedings of the Institution of Mechanical Engineers, Part B: Journal of Engineering Manufacture July 1, (2006) 220, 1077-1086.

[9] B. Caulfield, P. E. McHugh, S. Lohfeld: "Dependence of mechanical properties of polyamide components on build parameters in the SLS process". Journal of Materials Processing Technology, Vol. 182. (2007) No. 1-3, 477-488

[10] P. K. Jain, P. M. Pandey, P. V. M. Rao: "Effect of delay time on part strength in selective laser sintering". Advanced Manufacturing Technology, Vol. 43 (2009) No. 1-2, 117-126

[11] P. K. Jain, P. M. Pandey, P. Rao: "Selective laser sintering of clay reinforced polyamide". Polymer Composites, Vol. 31 (2010) No. 4, 732–743.

[12] R. D. Goodridge, M. L. Shofner, R. J. M. Hague, M. McClelland, M. R. Schlea, R. B. Johnson, C. J. Tuck: "Processing of a Polyamide-12/carbon nanofibre composite by laser sintering". Polymer Testing, Vol. 30 (2010) No. 1, 94-100

[13] A. C. Miller, J. C. Berg: "Effect of silane coupling agent adsorbate structure on adhesion performance with a polymeric matrix". Composites Part A: Applied Science and Manufacturing, Vol. 34 (2003) No. 4, 327-332

[14] http://www.specialchem4polymers.com/ SpecialChem, [Accessed 12. Feb. 2014].

[15] S. Shokoohi, A. Arefazar, R. Khosrokhavar: "Silane Coupling Agents in Polymer based Reinforced Composites; a review". Journal of Reinforced Plastics and Composites Vol. 27 (2008) No. 5, 473-485

[16] http://www.potterseurope.org/ [Accessed 10. Oct. 2014].

[17] S. Y. Fu, X. Q. Feng, B. Lauke, Y. W. Mai: "Effects of particle size, particle/matrix interface adhesion and particle loading on mechanical properties of particulate– polymer composites". Composites Part B: Engineering, Vol. 39 (2008) No. 6, 933-961.

[18] P. Mareri, S. Bastide, N. Binda, A. Crespy: "Mechanical behaviour of Polypropylene Composites Containing Fine Mineral Filler: Effect of Filler Surface Treatment". "Composites Science and Technology, Vol. 58 (1998) No. 5, 747-752

[19] British Standards Institution: BS ISO 17281: "Plastics — Determination of fracture toughness (G_{IC} and K_{IC})" At moderately high loading rates (1 m/s). London: British Standards Institute, 2002.